IOP Publishing Superconductor Science and Technology

Supercond. Sci. Technol. **31** (2018) 055016 (9pp) https://doi.org/10.1088/1361-6668/aab8c3

Improvements of fabrication processes and enhancement of critical current densities in (Ba,K)Fe_2As_2 HIP wires and tapes

Sunseng Pyon[1,5], Takahiro Suwa[1], Tsuyoshi Tamegai[1], Katsutoshi Takano[2], Hideki Kajitani[2], Norikiyo Koizumi[2], Satoshi Awaji[3], Nan Zhou[4] and Zhixiang Shi[4]

[1] Department of Applied Physics, The University of Tokyo, Hongo, Bunkyo-ku, Tokyo 113-8656, Japan
[2] Naka Fusion Institute, National Institutes for Quantum and Radiological Science and Technology (QST), 801-1 Mukoyama, Naka-shi, Ibaraki 311-0193, Japan
[3] High Field Laboratory for Superconducting Materials, Institute for Materials Research, Tohoku University, Sendai 980-8577, Japan
[4] Department of Physics, Southeast University, Nanjing 211189, People's Republic of China

E-mail: pyon@ap.t.u-tokyo.ac.jp

Received 13 January 2018, revised 5 March 2018
Accepted for publication 22 March 2018
Published 13 April 2018

Abstract

We fabricated (Ba,K)Fe_2As_2 superconducting wires and tapes using the powder-in-tube method and hot isostatic pressing (HIP). HIP wires and tapes showed a high value of transport critical current density (J_c) exceeding 100 kAcm^{-2} at $T = 4.2$ K and the self-field. Transport J_c in the HIP wire reached 38 kAcm^{-2} in a high magnetic field of 100 kOe. This value is almost twice larger than the previous highest value of J_c among round wires using iron-based superconductors. Enhancement of J_c in the wires and tapes was caused by improvement of the drawing process, which caused degradation of the core, formation of microcracks, weak links between grains, and random orientation of grains. Details of the effect of the improved fabrication processes on the J_c are discussed.

Keywords: superconducting wires and tapes, (Ba,K)Fe_2As_2, critical current density, powder-in-tube (PIT), hot isostatic pressing (HIP)

(Some figures may appear in colour only in the online journal)

Introduction

The discovery of iron-based superconductors (IBSs) in 2008 [1] has prompted a great interest in their application potentiality. Shortly after the discovery, IBS wires and tapes were fabricated and their properties have been steadily improved, as described in several review articles [2–7]. Among the various IBS materials, the 122-type $AEFe_2As_2$ (AE = Ba, Sr) [8, 9] are studied as most promising candidates for high-performance superconducting wires and tapes, since they have high transition temperature, T_c, (~38 K) for bulk [8, 9], very high upper critical field, H_{c2} (>500 kOe) [9–12], and relatively small anisotropy ($\gamma < 2$) [10–12]. Their large H_{c2} and small anisotropies make them attractive compared with MgB_2 having a $T_c \sim 39$ K [2, 13]. It has been demonstrated that the critical current density (J_c) in 122-type IBS single crystals exceeds 1×10^6 A cm^{-2} [14], and it can be enhanced further by introducing artificial defects [14–17]. These values exceed those of commercially available NbTi or Nb_3Sn wires. In addition, the values of the J_c of 122 wires/tapes/films are steadily increasing for practical use [7].

For practical use of superconducting wires, weak links between superconducting grains should be eliminated and the density has to be maximized. For these purposes, pressing superconducting wires is the most effective method. Principally, two pressing methods for the fabrication of IBS wires and tapes have been proven to be effective in enhancing J_c: namely, uniaxial pressing for tapes [18–22] and hot isostatic

[5] Author to whom any correspondence should be addressed.

pressing (HIP) for round wires [23–30]. Although the uniaxial-press method has realized the highest J_c value, it cannot be used for the fabrication of round wires. Round wires processed by the HIP technique are promising for high-field applications similar to the pressed tapes because their round shapes are much more advantageous and convenient than the textured tape for a wide range of applications. It should be noted that the HIP process has been proven to be very effective in enhancing the J_c of commercial Bi2223 tapes [31, 32]. At present, the reported highest value of transport J_c in both $(Ba,K)Fe_2As_2$ and $(Sr,K)Fe_2As_2$ HIP wires is 175 kA cm^{-2} under the self-field and 20 kA cm^{-2} under 100 kOe [29]. It is still lower than transport J_c in IBS tapes. Conditions for polycrystalline powder synthesis and wire-fabrication process of HIP wires should be optimized for future applications.

To enhance the J_c in the HIP wire, both high-quality polycrystalline materials and sophisticated wire-fabrication process are necessary. The importance of the quality of the core materials for J_c enhancement in superconducting wire has been demonstrated [29]. It is claimed that not only the heat treatment but also the mechanical deformation process in the fabrication of superconducting PIT wires and tapes affect the J_c [33]. To be specific, superconducting properties of the wire core are significantly damaged during the mechanical deformation process [29]. These results imply that improvements of mechanical fabrication processes for HIP wires are necessary for the enhancement of J_c. However, systematic analyses for the mechanical fabrication process in the HIP wire have not been reported.

In this paper, we focus on the HIP technique for the fabrication of $(Ba,K)Fe_2As_2$ superconducting wires and tapes, and their fabrication processes. $(Ba,K)Fe_2As_2$ superconducting wires and tapes are fabricated by PIT and HIP methods. Both transport and magnetic J_c are measured and compared for both HIP wires and tapes. We have achieved the largest value of J_c in the HIP wire under a high magnetic field of 100 kOe, which is almost twice larger than the previous record [29]. In addition, a relatively high value of J_c in the HIP tape is also achieved, which suggests that the HIP technique can be an alternative method to realize superconducting tapes with practical J_c. Remarkable enhancement of J_c is caused by the improvements of fabrication processes. Details of the effect of the fabrication process on J_c enhancement are evaluated by magnetization, magneto-optical (MO), and x-ray diffraction (XRD) measurements and are then discussed.

Experimental methods

Superconducting wires of $(Ba,K)Fe_2As_2$ were fabricated by the *ex situ* powder-in-tube (PIT) method. Polycrystalline powders of $Ba_{0.6}K_{0.4}Fe_2As_2$ were prepared by a solid-state reaction. The polycrystalline powder used is the same as that used in the previous work [29], and details of powder preparation are described in [29]. The ground powder was filled into a silver tube with outer and inner diameters of 4.5 mm and 3 mm, respectively. In the present study, Ag tubes filled with powder were cold drawn into a round shape with a diameter of ~1.2 mm using dies with circular holes. After cutting them into short pieces, one of the pieces was put into 1/8 inch copper tube and redrawn into a square shape with a groove roller down to a diagonal dimension of 1.2 mm. Furthermore, a part of the wire was deformed into a tape form with 0.4 mm in thickness. After the drawing process, both ends of the wire were sealed using an arc furnace. The sealed wires were sintered using the HIP technique. Wires and tapes were heated for 4 h at 700 °C in an argon atmosphere under different pressures of 0.1–175 MPa. HIP processes under the highest pressure 175 MPa were performed at National Institutes for Quantum and Radiological Science and Technology, and others were performed at the University of Tokyo. In order to evaluate transport J_c, a DC electric current up to 150 A was delivered through the wire at a ramping rate of 50–100 A min^{-1}. Measurements were performed in liquid helium to minimize the effect of Joule heating at the current leads. The critical current measurements in high magnetic fields were carried out by using the 15T-SM at the High Field Laboratory for Superconducting Materials, IMR, Tohoku University. Current–voltage (I–V) characteristics up to 140 kOe were measured by the four-probe method with a solder for contacts. Bulk magnetization at a low field of 10 Oe was measured by a superconducting quantum interference device magnetometer (MPMS-5XL, Quantum Design). Bulk magnetization in the range between –90 kOe and 90 kOe at a temperature of 4.2 K was measured by a Physical Property Measurement System (Quantum Design) using the vibrating sample magnetometer option. The filling factor of the core was estimated from the volume and weight of the cut and polished core of the wire. Vickers hardness, Hv, was measured on the polished surface of the wire core. For MO imaging, the HIP wire and tape were cut and the transverse cross sections were polished with lapping films. An iron–garnet indicator film was placed in direct contact with the sample and the whole assembly was attached to the cold finger of a He-flow cryostat (Microstat-HR, Oxford Instruments). MO images were acquired by using a cooled-CCD camera with 12-bit resolution (ORCA-ER, Hamamatsu). The phase identification and the evaluation of texturing of the core of the HIP wire were carried out by powder XRD with Cu-Kα radiation (Smartlab, Rigaku).

Results and discussions

Transport J_c in HIP wires and tapes was evaluated from their E-J characteristics under various magnetic fields in liquid helium (T = 4.2 K). We evaluated the transport J_c for the HIP wire by adopting the 1 μV cm^{-1} criterion. Except for more than ten wires that have been measured for their transport J_c, data showing the maximum J_c under magnetic fields is summarized in figure 1. Transport J_c in the $(Ba,K)Fe_2As_2$ HIP wire from our previous work, which was the highest value of transport J_c among IBS round wires, is also plotted for comparison [29]. The most important achievement is the highest transport J_c value among IBS superconducting HIP wires at a high magnetic field. As shown in figure 1(a), J_c under a magnetic field of 100 kOe reaches 38 kA cm^{-2}. This

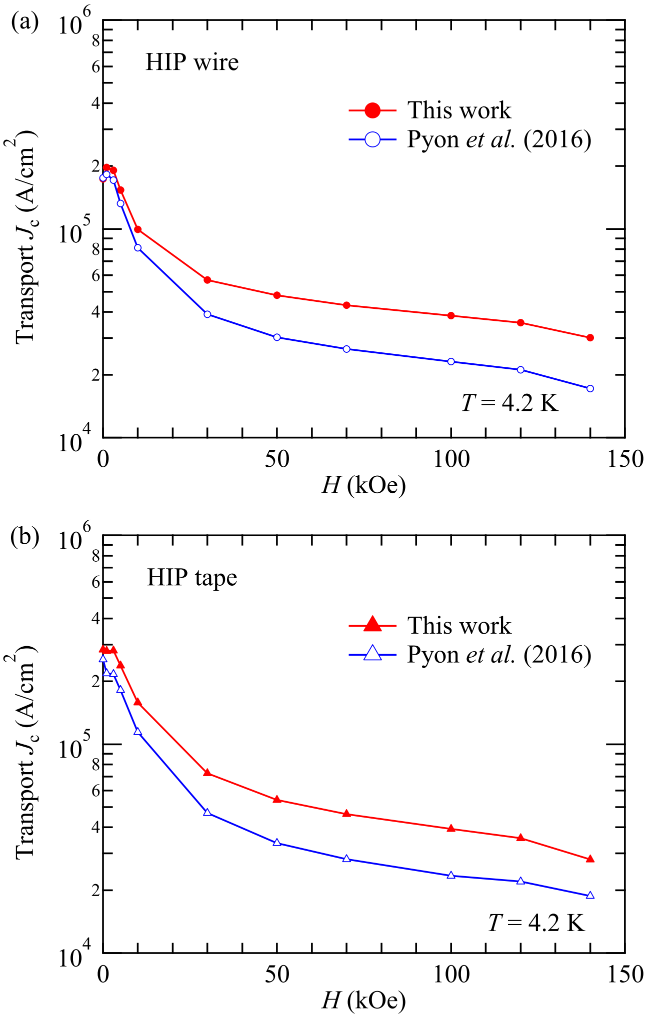

Figure 1. Magnetic field dependence of transport J_c in the $(Ba,K)Fe_2As_2$ HIP (a) wire and (b) tape at 4.2 K. Transport J_c in the $(Ba,K)Fe_2As_2$ HIP wire and tape from our previous publication are also plotted [29].

is almost twice larger than the previous highest value of J_c among round wires using iron-based superconductors [29]. The self-field transport J_c reaches 173 kA cm^{-2}, which is almost the same level compared with the highest record. It is noteworthy that the transport J_c under a magnetic field of 1 kOe reaches 196 kA cm^{-2}, which is larger than the J_c in the self-field. Such behavior was also discussed by Hecher *et al* and may be caused by grain size effect [28]. The HIP tape also shows high transport J_c, as shown in figure 1(b). The J_c of the HIP tape is higher than that of the HIP wire, and the transport J_c of the HIP tape has reached 283 kA cm^{-2} in the self-field, and 39 kA cm^{-2} in a magnetic field of 100 kOe. These values are also higher than the reported values in our previous work, and specifically, twice larger in the magnetic field of 100 kOe [29].

To evaluate the local J_c distribution in the core, we performed MO measurements on the HIP wire and tape. Figures 2(a) and (c) are optical images of the transverse cross sections of the HIP wire and tape, respectively. Copper, silver, and $(Ba,K)Fe_2As_2$ core regions are clearly identified and no voids are observed in these optical images. The shape of the core of the HIP wire is nearly square reflecting the groove rolling at the final drawing process. In the case of the HIP tape, a gourd-shaped core, where the center is a little thinner than the outer parts, is observed. This is very similar to our previous work [29]. Figures 2(b) and (d) show MO images of the transverse cross section of the core of the HIP wire and tape in the remanent state, respectively. These images are obtained at 5 K after applying 2 kOe along the wire axis for 0.2 s, which is subsequently reduced to zero. Figure 2(b) shows uniform and fully trapped magnetic flux distribution in the HIP wire. The bright region corresponds to the trapped flux in the sample. It demonstrates the presence of uniform bulk current flowing in the wire core across many grains. This indicates that weak links across grain boundaries are much improved by the high-pressure process compared with our previous $(Ba,K)Fe_2As_2$ PIT wire, which was processed at ambient pressure [34]. In the core of the HIP tape, although the almost uniform trapped field in the core region is similar to that in the core of the HIP wire, the central part is slightly less bright than the outer parts. As described in the previous report [29], a gourd-shaped core is harmful for the J_c because the central part has lower J_c probably due to stronger deformation. Figures 2(e) and (f) show the magnetic induction profiles along the red line in figures 2(b) and (d), respectively. Figures 2(e) and (f) show that, as the temperature is increased toward the T_c, the intergranular critical current in the HIP wire and tape decreases only gradually. Such behavior indicates that a uniform bulk current flows in the core across many grains in a broad temperature range below the T_c. These observations indicate the fact that weak links between grains are improved by sintering using the HIP technique.

The improvements of weak links by the HIP process are also suggested from the core density of HIP wires. We found that the sintering pressure has a clear correlation with the J_c, and the core density. Figures 3(a)–(c) show the sintering pressure dependence of the magnetic J_c, filling factor, and Hv, respectively. The magnetic J_c of the HIP wire and tape were evaluated from the irreversible magnetization using the extended Bean model [14]. The magnetic J_c, filling factor, and Hv show positive correlation with the sintering pressure. These results clearly show that high core density plays a key role in achieving the practical level of J_c, as discussed for IBS pressed tapes [18]. We have also estimated and compared both previous and present HIP wires sintered at 175 MPa. They have almost the same value of filling factor of 96%–97% and Hv of 243–247. By contrast, magnetic J_c under the self-field is slightly different. Magnetic J_c at the self-field in the present wire is 240 kA cm^{-2} and that in the previous wire is 207 kA cm^{-2}, respectively. Furthermore, as shown in figure 1, transport J_c in the present wire is twice larger than that in the previous wire at a high field of 100 kOe. These results imply that sintering pressure is not the only key parameter for increasing the J_c of HIP wires.

The present study demonstrates that our HIP wires and tapes show the highest transport J_c at high fields, which is twice larger than the previous record of HIP wires and tapes reported in [29], as clearly shown in figure 1. In addition,

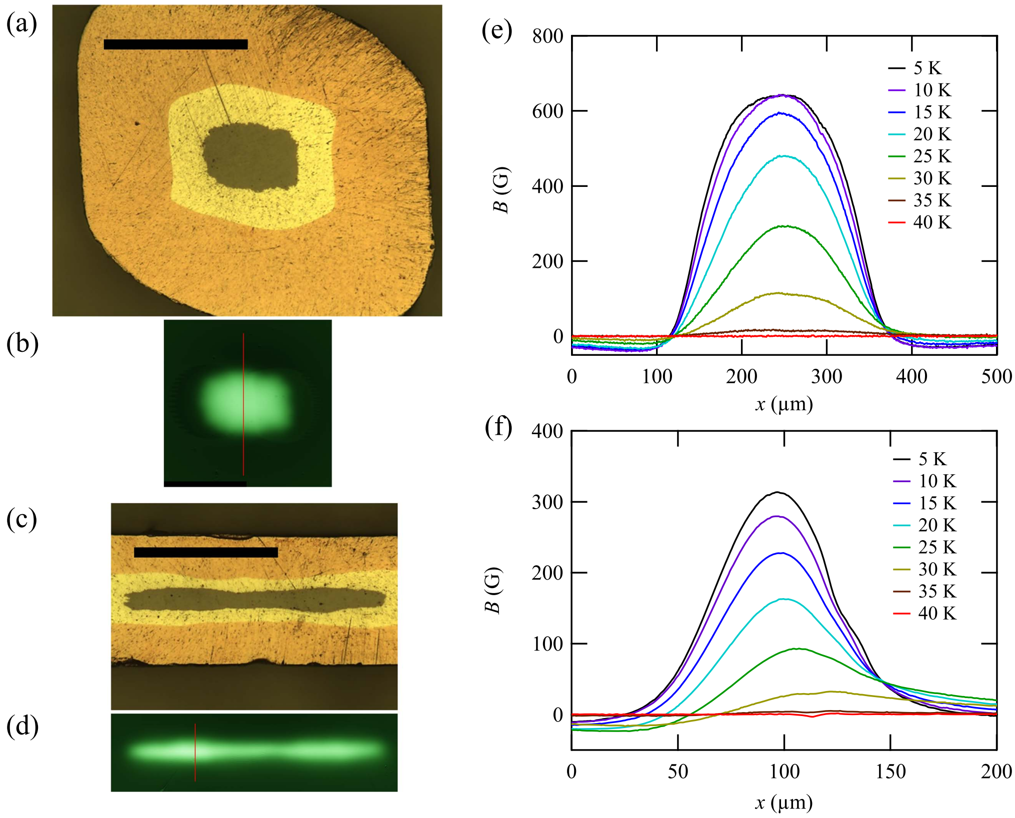

Figure 2. Optical micrographs of the transverse cross sections of the HIP (a) wire and (c) tape. Black bars indicate the length of 0.5 mm. Differential MO images of the core regions of (b) the HIP wire in (a) and (d) the HIP tape in (c) in the remanent state at 5 K after cycling the field up to 2 kOe for 0.2 s. (e) and (f) Local magnetic induction profiles at different temperatures taken along the red lines in (b) and (d), respectively.

well-connected grains, which realize large intergranular J_c, are demonstrated by MO images. Now, we discuss what the key factor is for the significant enhancement of J_c in HIP wires and tapes. In both the present and previous wires and tapes, the same polycrystalline powder and the same copper and silver tubes were used. Furthermore, conditions for the HIP process, such as sintering temperature, pressure, and time are also the same. In the present study, dies with circular holes were used in the intermediate drawing process. Therefore, the mechanical deformation processes for wires and tapes should strongly affect the J_c. This is similar to cold-pressed tapes, where mechanical process such as cold pressing before sintering affected the J_c, density of core, and texturing in the core [18]. We consider two possibilities concerning how the changes in the mechanical drawing process enhance J_c. First, the degree of degradation of the core could be different. Superconducting properties in the core of the wire are degraded through mechanical deformation and are improved through the sintering process [27]. It is possible that the degree of degradation depends on how the wires are deformed. The core of the wire was deformed by a more uniform force when the wire was drawn using dies with circular holes. On the other hand, it was deformed with less uniform force when the wire was groove-rolled with a square shape roller. If the degradation is suppressed by a more uniform mechanical deformation, higher J_c should be expected after sintering. Second, the state of the core of the wires and tapes, such as microcracks, weak links between grains, and the texturing of grains may be different. In the pressed tape, mechanical deformation before sintering affects the J_c. Gao *et al* reported that the practical level of J_c in the cold-pressed tape was realized by the high core density, higher texturing, and changes in the microcrack structure [18]. In the present HIP wires and tapes, it is expected that the density of the core is similar to the previous wire and tape, since they have not been pressed before sintering and the sintering conditions are the same. Actually, as shown in figure 3, densities of both the present and previous HIP-wire cores are quite similar. However, different drawing processes using dies with circular holes and subsequent groove rolling may induce different texturing, coupling between grains, and microstructures in the HIP wire and tape, similar to the case of pressed tapes. In the following paragraph, these possibilities are investigated through magnetization and x-ray analyses.

First, to evaluate the effect of the wire-fabrication process on superconducting properties in the core of the wire and tape, characteristics of (Ba,K)Fe_2As_2 wires and tapes used in our previous work [29] are compared. It should be noted that both wires and tapes are fabricated using the same batch of polycrystalline (Ba,K)Fe_2As_2 powders. The difference between this work and previous works is that while a groove roller was exclusively used in the previous work, dies with circular holes are used in the intermediated drawing process in the present study. Figure 4 shows the temperature

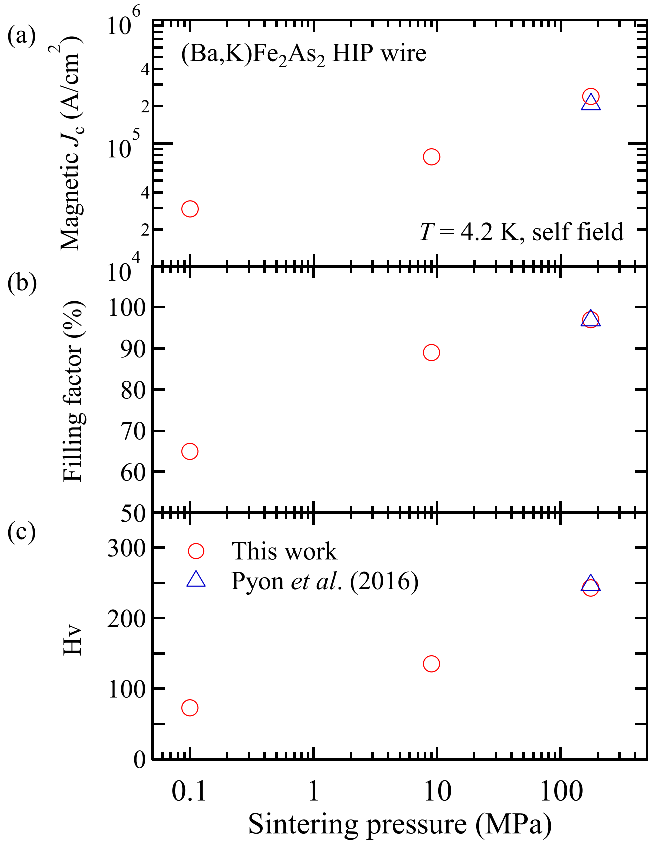

Figure 3. Sintering pressure dependence of (a) magnetic J_c at 4.2 K under the self-field, (b) filling factor of the core and (c) Hv in the $(Ba,K)Fe_2As_2$ HIP wires processed in different conditions. Data using HIP wire from our previous publication are also plotted [29].

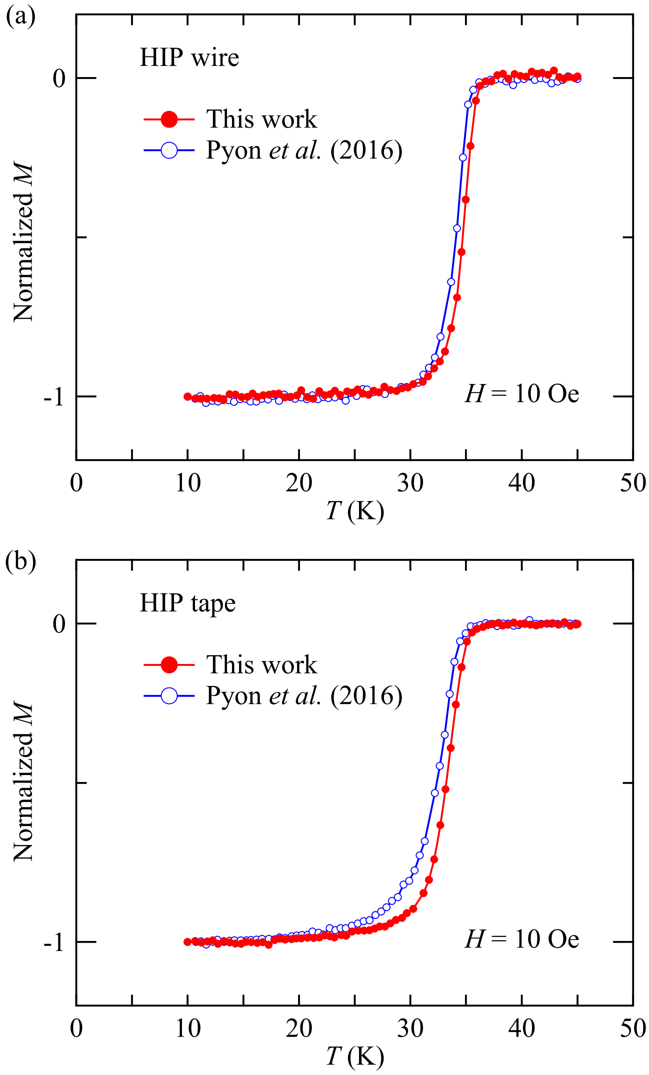

Figure 4. Temperature dependence of normalized magnetization at 10 Oe for the $(Ba,K)Fe_2As_2$ HIP (a) wire and (b) tape. The normalized magnetization in the $(Ba,K)Fe_2As_2$ HIP wire and tape from our previous publication are also plotted [29].

dependence of normalized magnetization for both the HIP wire and tape for this work and our previous work. The T_c in both the HIP wire and tape is approximately 37 K, although the T_c in polycrystalline raw materials is 38.2 K. The small reduction of T_c after the wire fabrication is also observed in the previous reports in the HIP wires [29]. This T_c reduction may be caused by degradation during the drawing process and incomplete recovery in the following sintering process, as discussed in [27]. It is noteworthy that the degree of T_c reduction depends on the wire-fabrication process. As shown in figure 4(a), the T_c in the HIP wire in this work is approximately 1 K higher compared with the previous wire. A similar tendency can be also found in HIP tapes, as shown in figure 4(b). Furthermore, a sharper drop of magnetization near the T_c is also observed in the HIP tape. Higher T_c and the sharper drop of magnetization near the T_c suggest more homogeneous carrier content. Considering the fact that the same powder was used for them, wire fabrication with more homogeneous force using dies is effective to suppress the degradation of the core during the drawing process and help recovery in the sintering process.

Second, to evaluate the degree of weak links, we performed analyses of magnetic J_c in the HIP wire and tape by magnetization measurements. From the anisotropy of magnetic J_c in the HIP tape, we can roughly evaluate the degree of the weak-link area or microcracks in the core of the tape [29, 35]. Magnetic J_c of the HIP wire and tape was evaluated from the irreversible magnetization using the extended Bean model [14]. Evaluated magnetic field dependence of magnetic J_c of the HIP tape at 4.2 K is summarized in figure 5(a). The field directions applied to the samples are also described in figure 5(a). In the HIP tape, we observed an anisotropy of magnetic J_c. The magnetic J_c reached almost 350 kA cm^{-2} at the self-field when the magnetic field is applied parallel to the tape surface. This is larger than transport J_c at a self-field of 280 kA cm^{-2}. On the other hand, when the magnetic field is perpendicular to the tape surface, magnetic J_c of 220 kA cm^{-2} is smaller compared with that for the field parallel to the tape surface and transport J_c. A similar anisotropy of magnetic J_c and the difference from transport J_c have also been reported in tapes of $(Ba,K)Fe_2As_2$ and $(Sr,Na)Fe_2As_2$, which may be caused by microcracks in the tape core which is formed along the wire direction [29, 35, 36]. Here, we defined the anisotropy of J_c, R, as the ratio of two kinds of J_c,

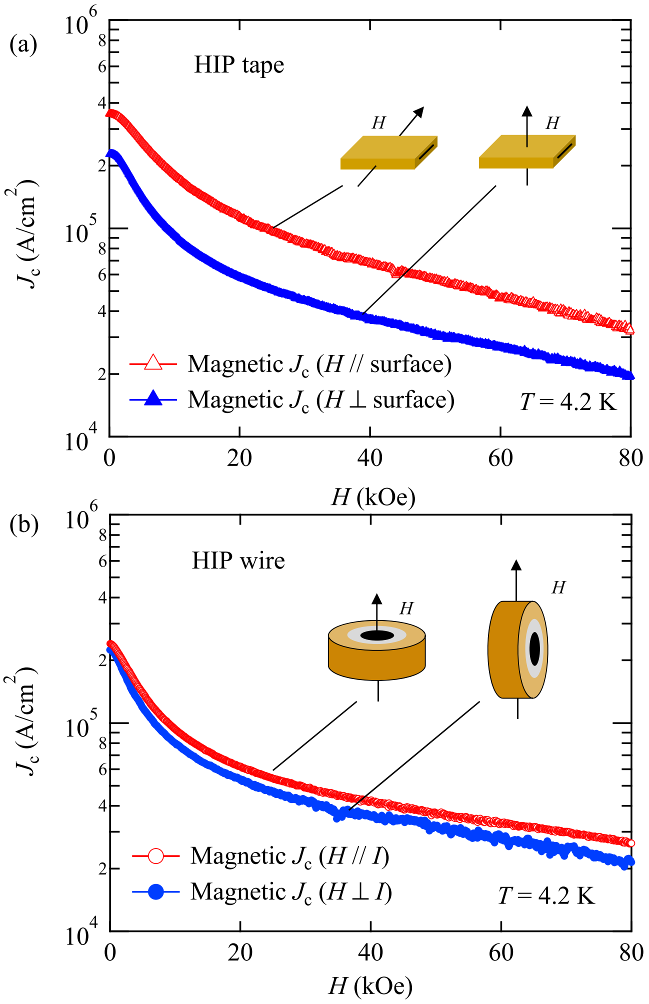

Figure 5. Magnetic field dependence of magnetic J_c in the (Ba,K)Fe_2As_2 HIP (a) tape and (b) wire at 4.2 K, respectively. Magnetic field is applied parallel and perpendicular to the tape surface for the HIP tape, and is applied parallel and perpendicular to the current flow direction for the HIP wire, as schematically drawn in the figure.

$J_c(H//\text{surface})/J_c(H\perp\text{surface})$. The R is approximately 1.5 in the present study. This value is smaller than $R \sim 2.0$ in the previous work [29]. This indicates that the weak link in the core of the HIP tape is improved by changing the fabrication process. Actually, the trapped field in the center of the HIP tape is not so much reduced as shown in the MO image in figure 2(d). We also applied the technique for the tape to wires to evaluate the degree of microcracks and their direction in the HIP wire. Field dependence of magnetic J_c in the HIP wire is also plotted in figure 5(b). The J_c in the HIP wire is comparable to but slightly lower than that of the tape. The anisotropy ratio R in the wire is slightly smaller than unity. This suggests that the degree of microcracks in the wire is smaller than that in the tapes. The value of R being less than unity implies that the direction of the microcrack is perpendicular to the direction of the current. This is consistent with the case of rolled tape, which was reported by Togano *et al* [37]. It is possible that microcracks, with their directions perpendicular to the current in the core of the wire, were developed in the drawing or groove-rolling process. The degree of microcracks may be controlled by reducing the speed of drawing, the core-reduction rate, and the pressure for sintering. By improving the wire-fabrication processes, there is still room for the enhancement of the J_c of the HIP wire.

Next, we discuss possible texturing in the core of the HIP wire using XRD. HIP wires were cut and polished to prepare two kinds of surfaces, which are parallel (longitudinal) and perpendicular (transverse) to the current direction, as shown in the inset of figures 6(a) and (b), respectively. XRD intensities for (002) and (103) peaks for two kinds of surfaces are shown and compared in figures 6(a) and (b). It should be noted that the intensity in the left part of figure 6(b) is multiplied approximately by 2.2 to normalize the incident x-ray intensity for the comparison with the right part of figure 6(b). This factor is evaluated from the diameter of collimated x-ray beams of 0.5 mm, and the major axis of the beam spot along the beam line on the wire surfaces is 42.5 mm ($2\theta = 13.5$) and 19.0 mm ($2\theta = 31.5$). When the x-ray is reflected by the surface parallel to the current, $r = I(002)/I(103)$ is $\sim$0.2, as shown in figure 6(a). On the other hand, when the x-ray is reflected by the surface perpendicular to the current, the intensity of the (002) peak is almost comparable to the noise level and the value of r is $\sim$0.02. In the case of pressed tapes, where grains are well-textured along the c-axis, the value of r becomes much larger than the unity [18, 22]. Reduction of the intensity of the (002) peak shown in figure 6(b) implies that the fraction of grains with their c-axis perpendicular to the current is reduced. 122-type materials are layered compounds and they usually show plate-like shapes. It is suggested that these grains in the core are orientated during the drawing and groove-rolling processes, although the degree of texturing is much weaker compared with tapes.

During fabrication processes such as groove rolling and drawing, plate-like grains could be concentrically textured, as shown by the yellow broken lines in figure 7(a). To determine the degree of texturing, we made a series of XRD measurements as the wire core is successively thinned down. The prepared surface is parametrized by α, as shown in figure 7(a). Namely, $\alpha = 1$ and $\alpha = 0$ correspond to the surface and the center of the core. The ratio of c-axis textured grains should be largest near the surface of the core, while it becomes smaller as the core is thinned toward the center. We calculated the α dependence of the ratio in the case of ideal concentric texturing, as shown in figure 7(b). Both in strong or weak textured situations, the ratio reduces with decreasing α. So, it is expected that the intensity of the (00 l) peaks is enhanced near the surface, while it is suppressed near the center. We repeated the polishing of the HIP wire, and the XRD measurements, alternately. The obtained XRD intensities of (002) peaks normalized to those of (103) are shown in figure 7(c). Actually, we confirmed this tendency in the data shown in figure 7(c). Near the surface of the core ($\alpha = 0.74$), the intensity of the (002) peak is the strongest. Calculated r values obtained from figure 7(c) are plotted as a function of α in figure 7(d). At $\alpha \sim 0.74$, r is the largest ($\sim$0.26). The general trend of r as a function of α is similar to the expected one, as shown in figure 7(b). This result also suggests that

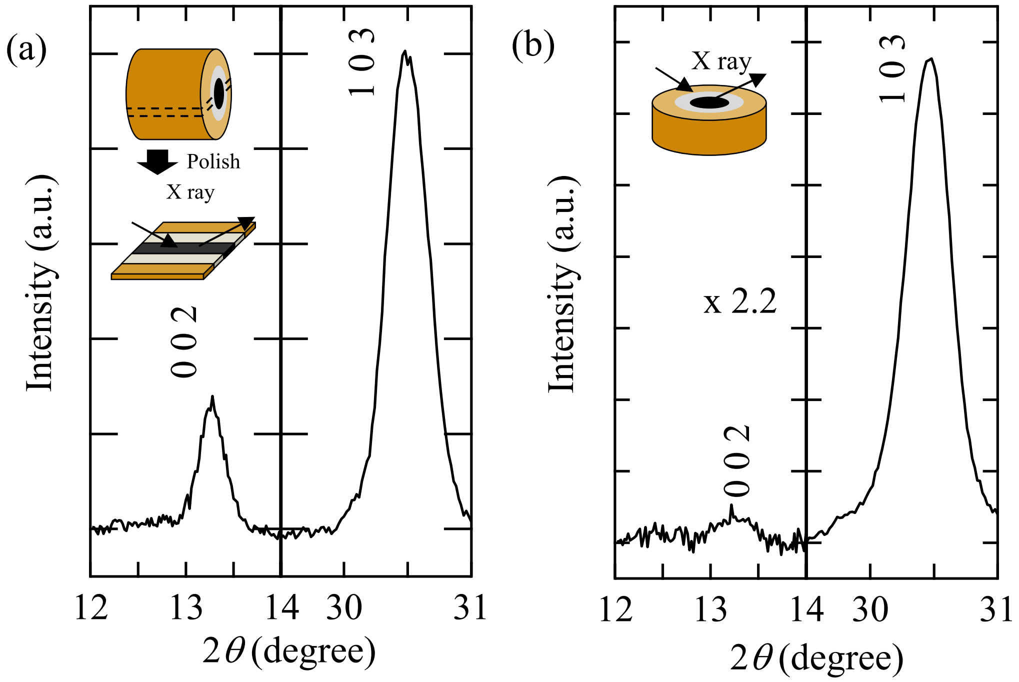

Figure 6. (a) (b) Powder XRD data of (002) and (103) peaks for two different cross sections of the HIP wires. Insets show the schematics of each cross section. Intensity in the left part of figure (b) is multiplied by 2.2 to normalize the incident x-ray intensity for the comparison with the right part of figure (b).

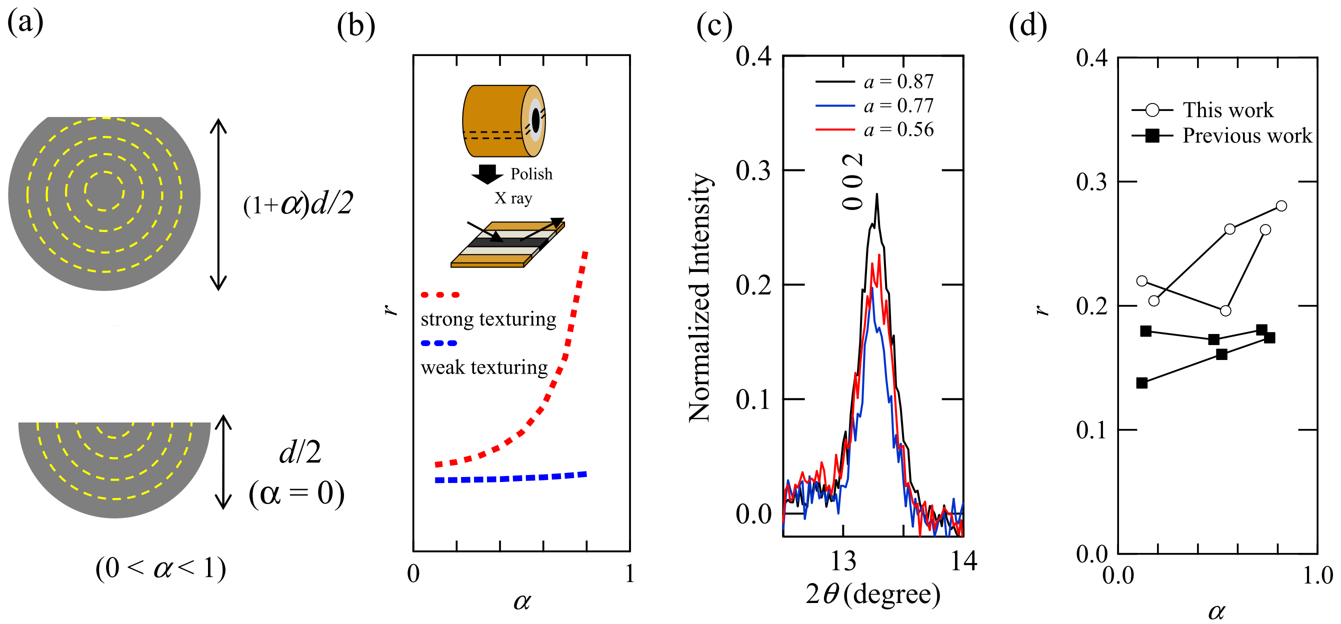

Figure 7. (a) Schematics of the core of polished HIP wires. d is the diameter of the core and α is the parameter that characterizes the exposed surface of the core. Yellow dotted lines indicate the possible texturing of grains in the core. (b) Simulated α dependence of the ratio of intensities of powder XRD peaks of (002) and (103), r, of the HIP wire. Inset shows the schematics of the cross section. (c) Normalized XRD intensity of (002) peaks of different surfaces of the core. (d) α dependence of r of the HIP wire. The data using the wire reported in our previous study are also shown [29].

grains in the core are orientated during the wire-fabrication process. We perform the same measurements using other pieces and confirmed that the trend is similar, as shown in figure 7(d). For comparison, the texturing in the core of HIP wires of our previous work [29] was also analyzed in the same manner, and the results are also shown in figure 7(d). Compared with the HIP wire in the present work, the value of r in the previous HIP wire is smaller. This implies that the degree of texturing is enhanced by the drawing process using dies compared with the groove-rolling process. The weaker texturing in the groove-rolled wire may be due to the less symmetric shape of the core.

Here, we summarize the improvements of the fabrication process. First, the degradation of the core of the wire and tape can be controlled to a certain extent by improving the mechanical deformation process. This is demonstrated by comparing the T_c in the present and previous wires and tapes in figures 4(a) and (b). Second, weak links between grains and microcracks, which are strongly related to the shape of the core imposed by the drawing process, reduce the J_c. Their effects on the J_c were clearly observed in the HIP tape in MO images as an anisotropy in the J_c, which are caused by their gourd-shaped cores. Weak links between grains should be improved by improving the shape of the core and controlling the drawing condition. Third, we demonstrate the partial texturing of the core in the HIP wire. The different J_c in the present and previous HIP wires may be caused by the different degree of texturing in the core. As suggested from the pressed tape of 122 compounds [18, 22] and round wire of Bi2212 [38], highly orientated grains in the core of the wire play a key role in increasing the J_c. The detailed mechanism regarding how the drawing methods can change the degree of orientation of the grain should be clarified.

Conclusion

We have fabricated the HIP wires and tapes using high-quality (Ba,K)Fe_2As_2 polycrystalline powders and with an improved mechanical drawing process using wire-drawing dies. They were characterized by magnetization, transport, and x-ray measurements as well as MO imaging. The HIP wires and tapes showed large values of transport J_c exceeding 100 kAcm^{-2} at $T = 4.2$ K and the self-field. In particular, transport J_c in the HIP wire reached 38 kAcm^{-2} in the high magnetic field of 100 kOe. This value is almost twice larger than the previous record of J_c in round wire using the same material. Enhancement of J_c in wires and tapes was caused by improving the fabrication process, in which dies with circular holes were used. This improvement is closely related to suppression of degradation of the core, microcracks, and weak links between grains as well as partial texturing. Further improvements of the mechanical deformation process for wires to induce higher texturing are important for further enhancement of J_c.

Acknowledgments

This work was partially supported by a Grant-in-Aid for Young Scientists (B) (16K17745), a Grant-in-Aid for Scientific Research (A) (17H01141), and the Japan-China Bilateral Joint Research Project by the Japan Society for the Promotion of Science (JSPS, the project number is 11611140101). This work was partially performed at the High Field Laboratory for Superconducting Materials, Institute for Materials Research, Tohoku University (Project No16H0045). We thank Z Gao, K Togano and H Kumakura for fruitful discussions for improving the quality of the polycrystalline sample.

ORCID iDs

Sunseng Pyon https://orcid.org/0000-0002-5716-1791

Reference

[1] Kamihara Y, Watanabe T, Hirano M and Hosono H 2008 *J. Am. Chem. Soc.* **130** 3296
[2] Ma Y 2012 *Supercond. Sci. Technol.* **25** 113001
[3] Shimoyama J 2014 *Supercond. Sci. Technol.* **27** 044002
[4] Ma Y 2015 *Physica* C **516** 17
[5] Pallecchi I, Eisterer M, Malagoli A and Putti M 2015 *Supercond. Sci. Technol.* **28** 114005
[6] Hosono H, Tanabe K, Takayam-Muromachi E, Kageyama H, Yamanaka S, Kumakura H, Nohara M, Hiramatsu H and Fujitsu S 2015 *Sci. Technol. Adv. Mater.* **16** 033503
[7] Hosono H, Yamamoto A, Hiramatsu H and Ma Y 2017 *Mater. Today* accepted manuscript (https://doi.org/10.1016/j.mattod.2017.09.006)
[8] Rotter M, Tegel M and Johrendt D 2008 *Phys. Rev. Lett.* **101** 107006
[9] Sasmal K, Lv B, Lorenz B, Guloy A M, Chen F, Xue Y-Y and Chu C-W 2008 *Phys. Rev. Lett.* **101** 107007
[10] Altarawneh M M, Collar K, Mielke C H, Ni N, Bud'ko S L and Canfield P C 2008 *Phys. Rev.* B **78** 220505(R)
[11] Yuan H Q, Singleton J, Balakirev F F, Baily S A, Chen G F, Luo J L and Wang N L 2009 *Nature* **457** 565
[12] Wang X–L *et al* 2010 *Phys. Rev.* B **82** 024525
[13] Braccini V *et al* 2005 *Phys. Rev.* B **71** 012504
[14] Nakajima Y, Tsuchiya Y, Taen T, Tamegai T, Okayasu S and Sasase M 2009 *Phys. Rev.* B **80** 012510
[15] Ohtake F, Taen T, Pyon S, Tamegai T, Okayasu S, Kambara T and Kitamura H 2015 *Physica* C **518** 47
[16] Tamegai T *et al* 2012 *Supercond. Sci. Technol.* **25** 084008
[17] Taen T, Ohtake F, Pyon S, Tamegai T and Kitamura H 2015 *Supercond. Sci. Technol.* **28** 085003
[18] Gao Z, Togano K, Matsumoto A and Kumakura H 2014 *Sci. Rep.* **4** 4065
[19] Lin H, Yao C, Zhang X, Zhang H, Wang D, Zhang Q, Ma Y W, Awaji S and Watanabe K 2014 *Sci. Rep.* **4** 4465
[20] Zhang X *et al* 2014 *Appl. Phys. Lett.* **104** 202601
[21] Gao Z, Togano K, Matsumoto A and Kumakura H 2015 *Supercond. Sci. Technol.* **28** 012001
[22] Lin H *et al* 2014 *Sci. Rep.* **4** 6944
[23] Weiss J D, Tarantini C, Jiang J, Kametani F, Polyanskii A A, Larbalestier D C and Hellstrom E E 2012 *Nat. Mater.* **11** 682
[24] Pyon S, Taen T, Ohtake F, Tsuchiya Y, Inoue H, Akiyama H, Kajitani H, Koizumi N, Okayasu S and Tamegai T 2013 *Appl. Phys. Express* **6** 123101
[25] Pyon S, Tsuchiya Y, Inoue H, Kajitani H, Koizumi N, Awaji S, Watanabe K and Tamegai T 2014 *Supercond. Sci. Technol.* **27** 095002
[26] Tamegai T, Pyon S, Tsuchiya Y, Inoue H, Koizumi N and Kajitani H 2015 *IEEE Trans. Appl. Supercond.* **25** 7300504
[27] Pyon S, Yamasaki Y, Kajitani H, Koizumi N, Tsuchiya Y, Awaji S, Watanabe K and Tamegai T 2015 *Supercond. Sci. Technol.* **28** 125014
[28] Hecher J, Baumgartner T, Weiss J D, Tarantini C, Yamamoto A, Jiang J, Hellstrom E E, Larbalestier D C and Eisterer M 2016 *Supercond. Sci. Technol.* **29** 025004
[29] Pyon S, Suwa T, Park A, Kajitani H, Koizumi N, Tsuchiya Y, Awaji S, Watanabe K and Tamegai T 2016 *Supercond. Sci. Technol.* **29** 115002
[30] Tamegai T, Suwa T, Pyon S, Kajitani H, Takano K, Koizumi N, Awaji S and Watanabe K 2017 *IOP Conf. Ser.: Mater. Sci. Eng.* **279** 012028

[31] Kobayashi S *et al* 2005 *IEEE Trans. Appl. Supercond.* **15** 2534
[32] Hayashi K 2011 *Jpn. J. Appl. Phys.* **50** 080001
[33] Malagoli A, Wiesenmayer E, Marchner S, Johrendt D, Genovese A and Putti M 2015 *Supercond. Sci. Technol.* **28** 095015
[34] Ding Q P, Prombood T, Tsuchiya Y, Nakajima Y and Tamegai T 2012 *Supercond. Sci. Technol.* **25** 035019
[35] Pyon S, Mine A, Suwa T and Tamegai T 2016 *Physica* C **530** 76
[36] Iyo A *et al* 2015 *Supercond. Sci. Technol.* **28** 105007
[37] Togano K, Gao Z, Taira H, Ishida S, Kihou K, Iyo A, Eisaki H, Matsumoto A and Kumakura H 2013 *Supercond. Sci. Technol.* **26** 065003
[38] Kametani F, Jiang J, Matras M, Abraimov D, Hellstrom E E and Larbalestier D C 2015 *Sci. Rep.* **5** 8285